Inhaled dry powder cisplatin increases antitumour response to anti-PD1 in a murine lung cancer model

Article *in* Journal of Controlled Release · December 2022

DOI: 10.1016/j.jconrel.2022.11.055

12 authors, including:

Tamara Davenne
InhaTarget Therapeutics
14 PUBLICATIONS **383** CITATIONS
SEE PROFILE

Pauline Percier Lehebel
InhaTarget Therapeutics
12 PUBLICATIONS **65** CITATIONS
SEE PROFILE

Lionel Larbanoix
Université de Mons
26 PUBLICATIONS **274** CITATIONS
SEE PROFILE

Oberdan Leo
Université Libre de Bruxelles
246 PUBLICATIONS **14,592** CITATIONS
SEE PROFILE

Journal of Controlled Release 353 (2023) 317–326

Contents lists available at ScienceDirect

Journal of Controlled Release

journal homepage: www.elsevier.com/locate/jconrel

Inhaled dry powder cisplatin increases antitumour response to anti-PD1 in a murine lung cancer model

Tamara Davenne [a,c,e,*], Pauline Percier [a], Lionel Larbanoix [b], Muriel Moser [c], Oberdan Leo [c], Etienne Meylan [c,d], Stanislas Goriely [c], Pierre Gérard [a], Nathalie Wauthoz [e], Sophie Laurent [b], Karim Amighi [e], Rémi Rosière [a,e]

[a] InhaTarget Therapeutics, Rue Antoine de Saint-Exupéry 2, Gosselies, Belgium
[b] Center for Microscopy and Molecular Imaging (CMMI), Université de Mons, Gosselies, Belgium
[c] Laboratory of Immunobiology, U-CRI, Université Libre de Bruxelles (ULB) Gosselies, Belgium
[d] Lung Cancer and Immuno-Oncology Laboratory, Bordet Cancer Research Laboratories, Institut Jules Bordet, ULB, Anderlecht, Belgium
[e] Unit of Pharmaceutics and Biopharmaceutics, Faculty of Pharmacy, ULB, Brussels, Belgium

ARTICLE INFO

Keywords:
NSCLC
Chemotherapy
Dry powder for inhalation
DPI
Immune checkpoint inhibitor
PD-L1

ABSTRACT

Despite advances in targeted therapies and immunotherapy in lung cancer, chemotherapy remains the backbone of treatment in most patients at different stages of the disease. Inhaled chemotherapy is a promising strategy to target lung tumours and to limit the induced severe systemic toxicities. Cisplatin dry powder for inhalation (CIS-DPI) was tested as an innovative way to deliver cisplatin locally via the pulmonary route with minimal systemic toxicities. In vivo, CIS-DPI demonstrated a dose-dependent antiproliferative activity in the M109 orthotopic murine lung tumour model and upregulated the immune checkpoint PD-L1 on lung tumour cells. Combination of CIS-DPI with the immune checkpoint inhibitor anti-PD1 showed significantly reduced tumour size, increased the number of responders and prolonged median survival over time in comparison to the anti-PD1 monotherapy. Furthermore, the CIS-DPI and anti-PD1 combination induced an intra-tumour recruitment of conventional dendritic cells and tumour infiltrating lymphocytes, highlighting an anti-tumour immune response. This study demonstrates that combining CIS-DPI with anti-PD1 is a promising strategy to improve lung cancer therapy.

1. Introduction

Despite progress in targeted therapy and immunotherapy, lung cancer remains the leading cause of cancer-related deaths worldwide, with non-small cell lung cancer (NSCLC) representing 85% of total cases [1]. Although the use of immune checkpoint inhibitors (ICIs) has been approved with great results in a limited subpopulation of NSCLC patients, a majority of patients still do not respond and develop resistances [2]. The use of ICI(s) with chemotherapy, has shown better efficacy than chemotherapy alone and thus is now considered a standard treatment option for patients with advanced lung cancer, non-eligible for targeted therapy [3–5].

Since its licensing in 1978, cisplatin has proven to be one of the most successful chemotherapeutic agents in the world [6,7]. Cisplatin is a first-generation platinum compound being used in the treatment against multiple cancers, including lung cancer [8]. This DNA-binding alkylating agent cross-links DNA strands, inhibiting DNA synthesis and thus leading to cell death of highly dividing cells, such as cancer cells [9]. In lung cancer patients, platinum doublets are commonly administered intravenously at the maximum tolerated dose (MTD) for 4 to 6 treatment cycles, requiring hospitalisation for the day (ESMO guidelines). Off-target toxicities on any non-cancer cell are a major challenge caused by intravenous (iv) administration of cisplatin. Nephrotoxicity is one of the main adverse events of cisplatin (dose-limiting toxicity), and it also causes ototoxicity, sensory neuropathy, as well as multiple hypersensitivity reactions [10]. Inhaled chemotherapy tackles the challenge of the severe systemic toxicities observed with the iv route [11].

Inhaled chemotherapy which includes inhaled cisplatin has been developed since 1968 but has only been administered by nebulizers in clinical research. Nebulizers present two major limitations in view of

* Corresponding author at: InhaTarget Therapeutics, Rue Antoine de Saint-Exupéry 2, Gosselies, Belgium.
E-mail addresses: tamara.davenne@inhatarget.com (T. Davenne), pauline.lehebel@inhatarget.com (P. Percier), lionel.larbanoix@umons.ac.be (L. Larbanoix), Muriel.moser@ulb.be (M. Moser), oberdan.leo@ulb.be (O. Leo), etienne.meylan@ulb.be (E. Meylan), stanislas.goriely@ulb.be (S. Goriely), nathalie.wauthoz@ulb.be (N. Wauthoz), Sophie.laurent@umons.ac.be (S. Laurent), karim.amighi@ulb.be (K. Amighi), remi.rosiere@inhatarget.com (R. Rosière).

https://doi.org/10.1016/j.jconrel.2022.11.055
Received 7 September 2022; Received in revised form 28 November 2022; Accepted 30 November 2022

delivering chemotherapy. First it causes major environmental contamination due to aerosol losses in the air and in the device, requiring full protective equipment for patients and investigators, as well as specific infrastructures at the hospital [12–15], considering the toxicity profile of chemotherapy compounds. Second, nebulization highly limits the amount of drug delivered and effectively deposited in the lungs. Indeed, in phase I nebulized cisplatin did not reach its dose-limiting toxicity due to administration time that were too long, a consequence of the limited solubility of cisplatin and the performance of the nebulizer [16]. Alternatively, dry powder inhalers (DPI) address these two limitations. DPIs are breath-activated inhalers allowing high drug doses to be deposited in the lungs within seconds with negligible contamination of the patient's environment by the powder aerosol [11]. This opens up the possibility of taking the inhaled chemotherapy at home and therefore of administering chemotherapy doses with high frequency, significantly improving quality of life [11].

Cisplatin dry powder for inhalation (CIS-DPI) was developed to address the current limitations of nebulized cisplatin in the clinic. C*IS*-DPI has been previously tested using solid lipid microparticles embedding cisplatin into a lipid matrix [17]. The formulation allows sustained release and retention of cisplatin in the lungs and increases drug exposure at the targeted tumour site, compared with cisplatin iv and nebulized solution [17,18]. Our previous work showed that CIS-DPI is well tolerated by mice when administered three times a week for two weeks at the MTD, as demonstrated by a thorough investigation of adverse reactions in the lungs and the kidneys [19].

The present study investigates the efficacy of CIS-DPI as a monotherapy and its combination with the ICI anti-PD1, which will be its future clinical position in NSCLC. This preclinical evaluation of treatment efficacy was performed using bioluminescent imaging, immunohistochemistry and the analysis of tumour-immune infiltrate.

2. Material & methods

2.1. Cell lines

The M109-luc2 mouse lung carcinoma cell line was previously described [17]. Cells were cultured in Roswell Park Memorial Institute (RPMI) 1640 (Sigma R8758) supplemented with 2 mM L-Glutamine for M109-luc2 cells. Cells used for in vivo implantation were cultured in the presence of 100 U of penicillin and 100 μg of streptomycin per ml (Lonza #DE17-602E).

2.2. Mouse strains and housing conditions

Six to eight week-old female BALB/cAnNRj mice were purchased from Charles River (Ecully, France) and were kept under conventional housing conditions (12 h/12 h night and day cycles, 22 ± 2 °C, 55 ± 10% relative humidity) and given dry food and water ad libitum. All experiments were performed in accordance with EU Directive 2010/63/EU for animal experiments and were approved by the local ethic committee (CEBEA) under approvals CMMI-201701 and 03 GOS CMMI.

2.3. Tumour model

The M109 orthotopic lung cancer model is derived from the M109-luc2 cell line, i.e., the M109-HiFR cell transduced with the luciferase reporter gene luc2 (pGL4.10[luc2] vector, Promega, Leiden, Netherlands). The orthotopic intrapulmonary implantation of M109-luc2 cells was previously described [20]. Briefly, under ketamine (Nimatek®)/xylazine (Proxylaz®) anaesthesia, mice were grafted with 1.4 million M109-luc2 cells suspended in 20 μL of a 50:50 *v*/v mix of HBSS/Matrigel (Corning® Matrigel®) and injected intercostally after incision of the skin and dissection of subcutaneous muscles. The intramuscular incisions were stitched with a 3–0 silk (Ethicon1, St-Stevens-Woluwe, Belgium) and 2 suture staples (Michel #BN507R) were used to close the skin incision. Mice were placed on a heating mattress and closely checked until complete recovery.

2.4. Cisplatin dry powder for inhalation (CIS-DPI)

C*IS*-DPI and blends used for mouse endotracheal administration were prepared according to the protocols described in our previous work [17]. Briefly, a previously-micronized cisplatin suspension (2% *w/v*, Umicore, Germany) was spray-dried in the presence of hydrogenated castor oil (1.98% w/v, Kolliwax, BASF) and tocopheryl polyethylene glycol succinate (0.02% w/v, Biomadys, France). The main characteristics of CIS-DPI obtained were in line with those previously reported and listed in Supplementary Table 1. Blends of the cisplatin spray-dried powder were then prepared in lactose monohydrate (Lactohale 300, DFE Pharma, Goch Germany) using a Turbula 2C motion mixer (Bachofen AG, Uster Switzerland) to appropriate cisplatin concentrations. Each blend was characterized for its cisplatin content and content uniformity. The results obtained were in line with those previously reported [17], with relative standard deviations (RSD) below 5% observed for all the CIS-DPI blends prepared, except the blend for the administration of 0.1 mg/kg cisplatin in the dose-range finding study (Fig. 1) for which an RSD of 12% was observed.

2.5. Treatment administration

On the third day post-cell engraftment (i.e., day 3), mice with no detectable bioluminescence were excluded and the remaining mice were randomly allocated to different treatment groups. The first treatment cycle started on day 7, which consisted of 5 consecutive days of CIS-DPI administration followed by 2 days of washout before starting the second treatment cycle. Adapted CIS-DPI lactose blends were used to deliver 1–2 mg powder to mice under isoflurane anaesthesia (4% and 2% isoflurane for initiation and maintenance, respectively) using an endotracheal device (Powder Administration Device for Animals, Aptar, France) according to the supplier's protocol. The murine anti-PD1 monoclonal antibody (clone RPM1–14 #BP0146, BioXcell) was diluted in PBS to administer 200 μL intraperitoneally at 10 mg/kg twice a week to mice [21].

2.6. Bioluminescence imaging

In vivo bioluminescence imaging (BLI) of mice was performed twice a week to follow tumour growth over time. BLI was performed by means of a Photon Imager Optima (Biospace Lab, France) that dynamically counted the emitted photons for at least 25 min while animals were under anaesthesia (4% and 2% isoflurane for initiation and maintenance, respectively) and after subcutaneous administration of 150 mg/kg of D-luciferin (Promega). Image analysis was performed with M3Vision software (Biospace Lab). Regions of interest were drawn on the mouse thorax, and signal intensities were quantified individually for a 5 min of the maximum signal intensity plateau.

2.7. Survival analysis

For survival analysis, day zero is always the day of the tumour graft. The date of death corresponds to the day an animal reached one of the humane endpoints described in the ethical protocol. When an animal died following the bioluminescence procedure or when it reached humane endpoints, an additional day was considered in the counting. Some animal died without reaching humane endpoints, in this case the date of death corresponds to the day the animal was found (considering a daily follow up was assured throughout the study).

2.8. Immunohistochemistry

Lung tissues were fixed in neutral buffered formaldehyde 4%,

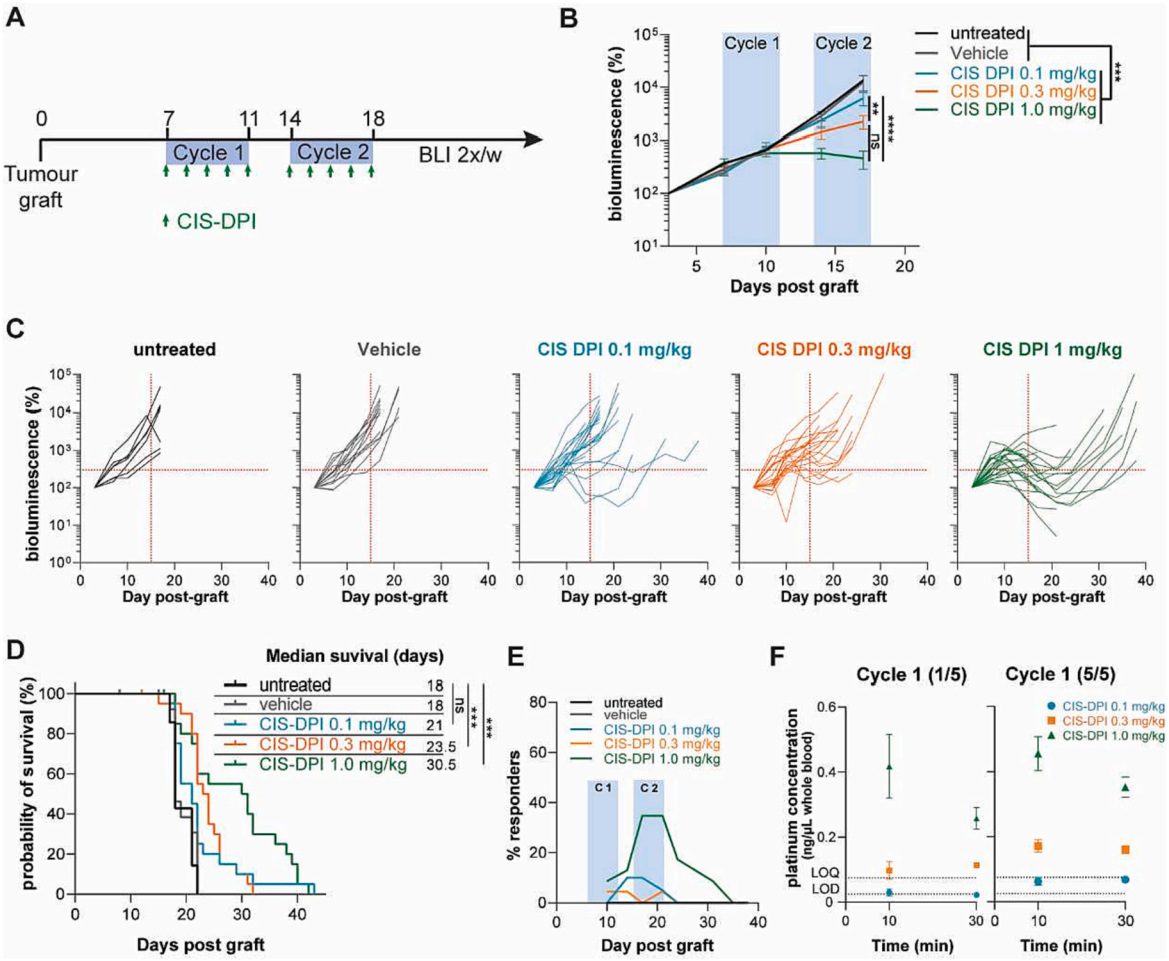

Fig. 1. Dose-dependent cytotoxicity of CIS-DPI in vivo (A) Treatment scheme of M109 tumour-bearing mice. The first cycle of administration of CIS-DPI starts on day 7 with 5 consecutive days of treatment followed by two days off (cycle 1); cycle 2 starts on day 14 for 5 consecutive days (bioluminescence = BLI). (B) Tumour growth was measured by bioluminescence and expressed as % of signal measured at day 3, represented as a mean ± SEM. Untreated controls ($n = 7$), vehicle controls ($n = 15$), CIS-DPI 0.1 mg/kg ($n = 18$), CIS-DPI 0.3 mg/kg ($n = 22$) and CIS-DPI 1 mg/kg ($n = 23$). Statistic are two-way ANOVA multiple comparisons between groups at day 17. (C) Tumour growth (% day 3) per group, lines represent individual mice. (D) Kaplan-Meier survival curves and median survivals of mice shown in (B—C). Survival statistics are Grehan-Breslow-Wilcoxon test between two groups (treated group vs untreated). The Bonferroni correction method was used to set the p value, considering $K = 4$ $p < 0.0125$. The absence of star is a non-significant difference (*$p < 0.05$,**$p < 0.01$, ***$p < 0.001$). (E) At every time point, the proportion of responders in each group was calculated and plotted. An animal is considered responder if it has a BLI signal below 150% (100% being the signal at day 3). (F) Platinum exposure in whole blood measured at 10 and 30 min following the first and the last CIS-DPI administration of the first treatment cycle (cycle 1). Dots represent means ± SEM ($n = 5$–6).

embedded in paraffin wax and sectioned at 4 µm. CD3 immunohistochemistry (IHC) was performed on a Ventana Discovery XT (Roche Diagnostics) using the ChromoMap detection system, using a rabbit monoclonal anti-CD3 (clone 2Gv6, Roche). Slides were counterstained with haematoxylin CD8 and PD-L1. After antigen retrieval using EnVision FLEX Target Retrieval High pH Solution (Tris/EDTA, pH 9; Agilent) for 30 min and 40 min at 97 °C respectively and peroxidase blocking, rabbit monoclonal anti-CD8α (clone D4W2Z; Cell Signaling) and rabbit monoclonal anti-PD-L1 (clone D5V3B; Cell Signaling) were used. Ki67 IHC was performed on a Ventana Discovery XT (Roche Diagnostics) using the DABMap detection system, using a rabbit monoclonal anti-Ki67 (clone clone 30–9, Roche). All slides were digitized at 20× with a NanoZoomer S360 scanner (Hamamatsu). The Visiopharm software package (Visiopharm) was used to delineate tumoral regions of interest within lung tissue sections manually, and to quantify IHC markers of interest in those regions. After applying Visiopharm's colour deconvolution algorithm to split the whole slide images into their separate haematoxylin & diaminobenzidine staining components, positively marked pixels were identified and labelled using a simple intensity threshold. For IHC markers with membrane expression (CD3, CD8, PD-L1), the computed Labelling Index (LI) is the percentage of immunostained (i.e. positively marked) tissue area. For the nuclear marker Ki67, the proliferating index corresponds to the percentage of positive area divided by the total area (positive + negative). In either case, LI values increase with the proportion of cells/area positively tagged for the considered marker.

2.9. Ex vivo tumour processing

On collection day, mice were euthanized by dislocation of the neck. Tumour were isolated, weighted and placed in digestion media which consisted of culture medium with 400 µg/mL DNase I and 20 µg/mL liberase TL™ (Merck #11284932001 and #5401020001). Tumours were grossly cut into pieces and incubated for 30 min at 37 °C. Tumour pieces were then transferred onto a 70 µm cell strainer and mashed with a syringe plunger. The resulting cell suspension was centrifuged; the pellet was resuspended and normalised at 200 mg/mL in RPMI. Finally, 50 µL (± 3 million cells) was transferred in a well of a 96-well plate for staining.

2.10. Flow cytometry staining

Cells were washed with PBS, blocked with Fc Block (BD biosciences # 553142) and stained with the fixable viability dye Viakrome 808 (Analis #311139) for 20 min at 4 °C. Two-time concentrated antibody mix was prepared in Brilliant stain buffer (BD biosciences #563794) and added directly to the cells. Cells were incubated for 20 min at 4 °C and then acquired on a Cytoflex LX (Beckman Coulter). Analysis of the flow cytometry data was performed with FlowJo V10.8.1. To obtain absolute counts, cell numbers obtained in a specific volume during acquisition were normalised per milligram of tumour tissue. Antibodies were purchased from BD biosciences (CD45 #564279, Ly6G #741813, TCRβ #562839, MHC II #566086, CD103 #564320, CD11b #740861, Ly6C #553104, F4/80 #565410, CD86 #560582, CD80 #560016, CD11c #565872, Ki67 #563757, PD1 #562523, CD4 #560582, CD4 #560582 and CD8 560,182). CD19 antibody was from ebiosciences #15391020.

2.11. Statistical analysis

GraphPad PRISM® version 9 software was used for statistical analysis. The Gehan-Breslow-Wilcoxon test with the Bonferroni correction was used to compare groups for survival analysis. Two-way ANOVA multiple comparisons were used to analyse mean tumour growth over time. Results are presented as the mean value ± SEM, unless otherwise indicated.

3. Results & discussion

3.1. Inhaled cisplatin induces dose-dependent anti-tumour activity in vivo

We previously showed that CIS-DPI improves response rate and prolonged survival when added to platinum doublets chemotherapy in preclinical studies [17]. In this study, CIS-DPI was tested at different cisplatin dose levels in the M109-luc2 lung carcinoma model to evaluate its dose-response efficacy. Mice were administered CIS-DPI for 2 treatment cycles, each consisting of 5 consecutive days of endotracheal drug administration followed by a two-day washout allowing the animals to recover (Fig. 1A). Due to repeated anaesthesia and the endotracheal procedure, some weight loss was observed during treatment cycles and thus treatments were limited to two cycles (about 10% loss after two treatment cycles, Fig. S1A).

Tumour growth was followed by in vivo bioluminescence imaging (BLI) at regular time intervals. BLI is a non-invasive imaging technique where the intensity of the signal correlates with tumour growth [21–23]. A highly significant reduction ($p < 0.001$) in tumour growth in all three CIS-DPI treated groups (0.1, 0.3 and 1 mg/kg) was observed when compared to the vehicle and the untreated groups (Fig. 1B-C). Moreover, a dose-dependent response was observed, with the strongest effect observed at the highest dose of 1 mg/kg cisplatin, which we previously set as the MTD [19]. Strikingly, the effect on tumours was rapid as the growth curves started separating before the end of the first treatment cycle, demonstrating the immediate antiproliferative action of cisplatin. CIS-DPI significantly increased survival rate over time at 0.3 and 1 mg/kg compared to untreated and vehicle groups (Fig. 1D). Specifically, the median survival was prolonged by +59%, from 18 days in the untreated and vehicle groups to 30.5 days in the CIS-DPI 1 mg/kg group (Fig. 1D). In that same group, there were up to 40% responders on day 20, while this percentage was lower at the two lower dose levels (Fig. 1E). Platinum was detected in blood 10 and 30 min post-administration, with concentrations directly proportional to the dose level. The platinum concentrations in plasma after the first CIS-DPI administration (Fig. 1F, Cycle 1/5) matched the previously reported concentrations following a single CIS-DPI administration in healthy mice [17]. Notably, only a minor increase in platinum plasma levels was observed on the last day of the treatment cycle (5/5), confirming the limited systemic exposure to cisplatin following repeated CIS-DPI administrations compared with iv cisplatin [17]. Inhaled cisplatin is mainly cleared from the organism though the kidney and eliminated in the urine, similarly to cisplatin iv. At the same cisplatin dose, we therefore estimate the clearance of platinum by urine following CIS-DPI being comparable to that of cisplatin iv [19].

Altogether, the results demonstrate a dose-dependent antitumour activity of CIS-DPI on M109 lung tumours, resulting in tumour shrinkage and prolonged survival rates. Dosing at 1 mg/kg five times a week was the most potent CIS-DPI regimen and was therefore used in future experiments. The use of a dry powder inhaler offers the possibility to deliver a smaller dose of chemotherapy every day compared with conventional systemic chemotherapy and opens the door to metronomic chemotherapy (MCT). MCT consists of repeated low-dose cytotoxic drugs with short or no drug-free breaks over prolonged periods [24]. Cisplatin MCT previously showed anti-angiogenic effects in vivo, with tumour growth reduction and reduced body weight loss compared to MTD cisplatin in hepatocarcinoma [25]. A recent review on MCT in NSCLC concluded that MCT showed lower toxicity and higher tolerability although its superiority to conventional chemotherapy was not fully verified [26]. Administration of CIS-DPI with high frequency (e.g., daily administration) leading to low systemic exposure [17], low immunosuppression [27] and therefore in favour of an immune-related antitumour response, has consequently many similarities with MCT. Therefore, our results suggest that CIS-DPI would be a good candidate for MCT-like therapy in NSCLC.

3.2. Cisplatin induces upregulation of PD-L1 on lung cancer cell lines and subsequent tumour infiltration by T cells

Next, we wanted to determine the effect of CIS-DPI on PD-L1 expression in M109 lung tumour. PD-L1 stands as a critical biomarker which helps predict response to anti-PD1/anti-PDL1 therapies and guides treatment decisions in NSCLC [28,29]. Cisplatin was shown to upregulate PD-L1 in lung tumours including in NSCLC patients [30]. To test the impact of CIS-DPI treatment on PD-L1 expression, PD-L1 staining was performed by IHC upon one cycle of treatment with CIS-DPI at 1 mg/kg. A trend of PD-L1 upregulation ($p = 0.061$) was observed on M109 tumours following one treatment cycle (Fig. 2A-B). Moreover, a significant increase of CD3 and CD8 staining was detected on the same samples (Fig. 2C-D), corresponding to the recruitment of CD8 tumour infiltrating lymphocytes (TILs). Together, these data show the upregulation of PD-L1 and TIL recruitment upon CIS-DPI treatment. This observation correlates with the PD-L1 upregulation following neoadjuvant cisplatin chemotherapy observed in NSCLC patients [30]. In this study, the percentage of PD-L1 positive tumour cells increased 2.5 fold after cisplatin treatment. Therefore, CIS-DPI shows a similar potential to induce PD-L1 upregulation (with ±3 fold induction) than observed in patient's tumour after administration of intravenous chemotherapy. Interestingly, CIS-DPI induced an upregulation of CD8+ cells in lung tumours, while there was no significant increase in NSCLC patient post administration of intravenous cisplatin [30]. TIL recruitment shows that CIS-DPI not only has a direct antiproliferative effect but also has an immunogenic effect. PD-L1 upregulation indicates that CIS-DPI treated tumours will favour a response to ICI therapies, such as anti-PD1 [29–31].

3.3. CIS-DPI improves anti-PD1 therapy

To test whether CIS-DPI had any additive effect to immunotherapy, CIS-DPI was combined with anti-PD1 administration. M109-bearing mice received two cycles of treatment (Fig. 3A). A heterogeneous response to anti-PD1 monotherapy was observed with 2/11 long survivors with no BLI signal up to day 64 (Fig. 3B-D). In comparison to untreated conditions, tumour growth on day 21 was significantly lower in the anti-PD1 and the combination groups. Moreover, on day 24, a significant reduction of tumour growth was observed between the

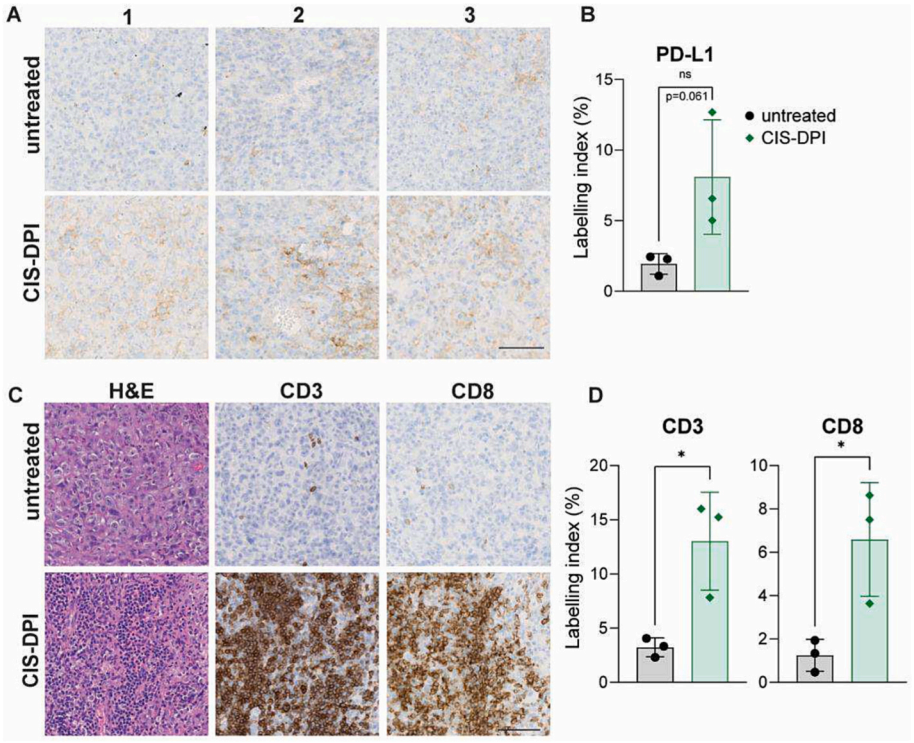

Fig. 2. CIS-DPI induces regulation of PD-L1 in lung tumours (A) Immunohistochemistry with anti-PD-L1 on M109 tumours at D14 (3 days after the last dose treatment dose of cycle 1) untreated or treated with CIS-DPI 1 mg/kg (n = 3 per group). Numbers [1–3, and] correspond to different tumours. Scale bar is 100 μm. (B) Quantification of PD-L1 expression on M109 tumours shown in (A). Results are expressed as labelling index (Percentage of labelling index = 100*area positive/(area positive+ area negative+ area other). Each symbol represents one tumour sample. (C) Immunohistochemistry showing H&E, anti-CD3 or anti-CD8 staining in one representative example in the untreated group and in the CIS-DPI group. Scale bar is 100 μm. (D) Quantification of CD3 and CD8 expression on M109 tumours shown in (C). Statistical analysis are unpaired t-tests FOR (B) and (D).

combination group compared with the anti-PD1 monotherapy (Fig. 3B-D). Interestingly, the effect of the combination treatment on tumour growth was more rapid than in the anti-PD1 group, with quantifiable differences from the untreated controls after the first treatment cycle. This shows the direct cytotoxic effect of cisplatin on the tumour, as previously observed (Fig. 2C) prior to the immune-related antitumour activity. Representative images of three mice from each group are shown in Fig. 3F. Tumours from the combination group shrunk significantly more than in the anti-PD1 group while all the untreated animals were dead by day 25. In addition, the CIS-DPI + anti-PD1 combination significantly prolonged the median survival from 24 to 33 days (+57%) when compared to the anti-PD1 monotherapy (Fig. 3E). The percentage of responders (a responder is defined as having a signal below 150%, 100% representing each animal signal on day 3) was up to 75% in the combination group (versus only 27% in the anti-PD1) after the two treatment cycles before decreasing due to the discontinuation of treatment cycles (Fig. 3G). It suggests that additional treatment cycles could further prolong the high response rates. Unfortunately, this was not possible using endotracheal administration for the reasons previously mentioned. The presence of a long survivor in the combination and in the anti-PD1 group suggested a durable anti-tumour immune response in these two groups. Altogether these data demonstrate a significant additive effect of CIS-DPI on the anti-PD1 therapy in terms of tumour growth reduction and prolonged survival. This is explained by the immediate antiproliferative effect of the cisplatin and its immunogenicity, which together with the immune checkpoint inhibitor anti-PD1 permit an anti-tumour immune response.

3.4. Combination of CIS-DPI ± anti-PD1 increases the number of intratumoral dendritic cells subset DC1

To demonstrate the immunogenicity of CIS-DPI and its impact on the anti-tumour immune response when combined with anti-PD1, the tumour immune infiltrate was analysed. M109 tumour-bearing mice were either left untreated, or treated with CIS-DPI, anti-PD1 or the combination of CIS-DPI and anti-PD1 for one cycle. Tumours were harvested two days after the last CIS-DPI administration (day 13), digested and analysed by flow cytometry to monitor innate immune cell populations (Fig. 4A, Fig. S1B).

Mice treated with CIS-DPI and CIS-DPI + anti-PD1 displayed a reduced tumour weight when compared to the other experimental groups (Fig. 4B), in agreement with the rapid cytotoxic effect of cisplatin, as previously documented (Fig. 3B, D and G).

There were significantly more hematopoietic $CD45^+$ cells in the anti-PD1 monotherapy group compared to the untreated controls or to CIS-DPI monotherapy, corresponding to intratumoral immune cell infiltration (Fig. 4C). Although there were no changes in the numbers of tumour associated macrophages ($F4/80^+$) between groups, these cells were expressing significantly high levels of the activation marker MHC II in the anti-PD1 and in the combination groups, compared with untreated control and the CIS-DPI monotherapy group (Fig. 4D-E). Another activation marker, CD86, was also significantly upregulated, specifically in the combination group (Fig. 4F), suggesting a possible polarization of these cells toward an M1-like, proinflammatory phenotype [31]. Murine conventional dendritic cells (cDCs) can be classified as DC1 when expressing the CD103 marker and as DC2 when expressing CD11b [32]. In the combination group, a significantly higher proportion and number of DCs belonged to the DC1 subset (Fig. 4G-H). cDC1s are potent inducers of cellular immunity due to their efficient processing and cross-presentation of tumour antigens on MHC class I molecules to activate T cells [32]. The expression (mean fluorescence intensity) of the activation markers MHC II and CD86 did not change at the surface of DC1 cells (Fig. I-J). In contrast, a significantly smaller proportion of DCs was from the DC2 subset in the combination group, although their numbers in the tumour were unchanged (Fig. 4K-L). Therefore, the increase is due to DC1 recruitment to the tumour site. Surprisingly, DC2 expressed significantly more CD86 and MHC II specifically in the CIS-DPI monotherapy compared to the other groups (Fig. 4M-N). CD86 is a co-stimulatory molecule and therefore its upregulation on DC2 by CIS-DPI reflects the activation of this subset by the CIS-DPI. In sum, these results revealed the hallmark of an anti-tumour immune response upon anti-PD1 treatment, which was further enhanced by CIS-DPI. This immunomodulatory effect of cisplatin has been reported after a single dose in breast cancer, correlating our observations with CIS-DPI [33].

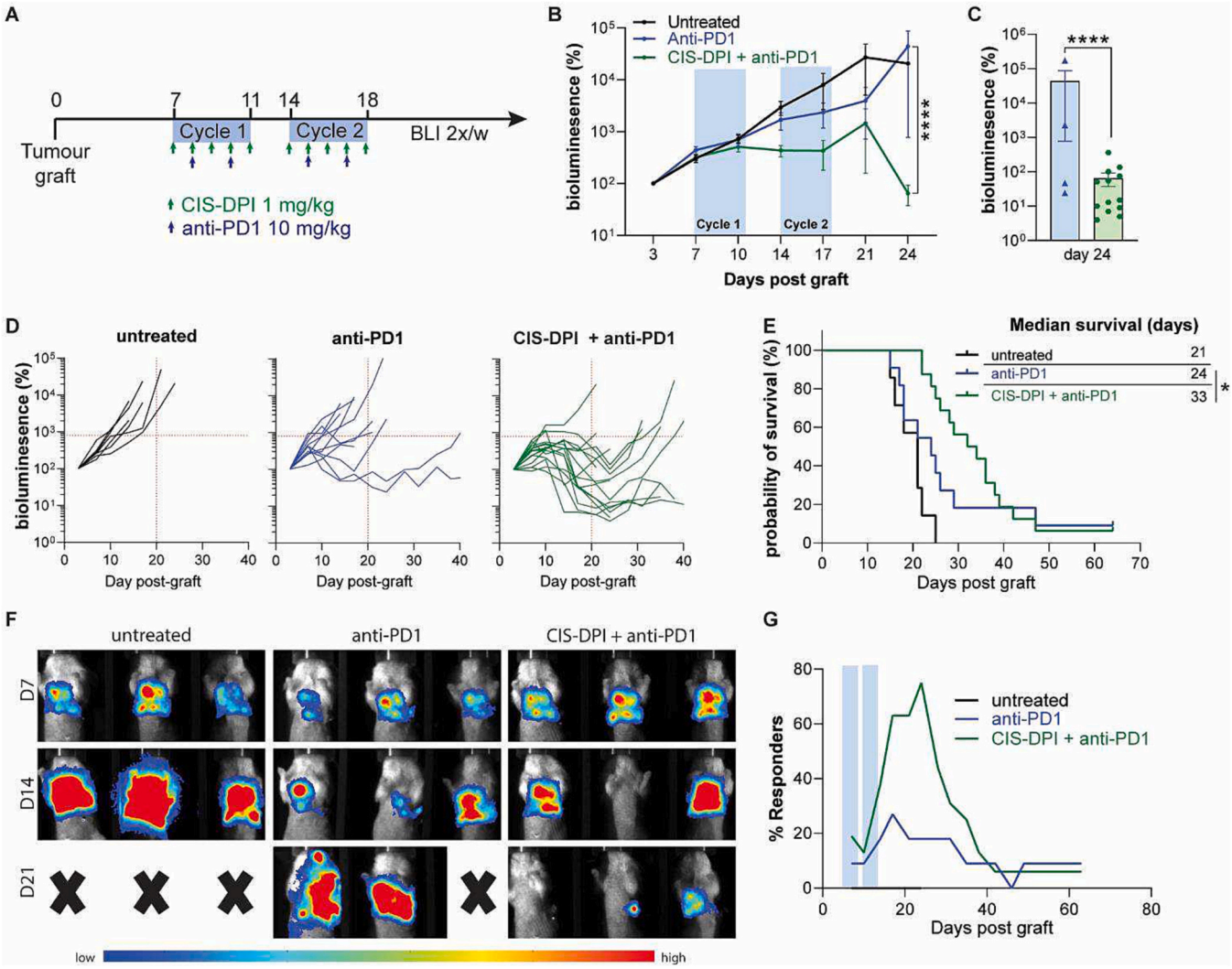

Fig. 3. CIS-DPI improves anti-PD1 therapy. (A) Treatment scheme of M109 tumour-bearing mice. The first cycle of administration of CIS-DPI starts on day 7 with 5 consecutive days of treatment followed by two days off (cycle 1); cycle 2 starts on day 14 for 5 consecutive days (bioluminescence = BLI, was performed twice a week). The anti-PD1 treatment was administered twice a week on indicated day at 10 mg/kg (bioluminescence = BLI). (B) Tumour growth measured by bioluminescence was expressed as percentage (%) of signal measured on day 3. Mice were left untreated (n = 7) or received the; anti-PD1 ($n = 11$) or the combination treatment CIS-DPI 1 mg/kg + anti-PD1 ($n = 16$). Lines represent mean ± SEM. Statistics are two-way ANOVA multiple comparisons on day 24 (B—C). (C) Individual tumour growth values (% day 3) ± SD of mice in anti-PD1 and combination groups at day 24. (D) Individual tumour growth expressed as percentage of day 3 signal of mice shown in (B—C). (E) Kaplan-Meier survival curves and median survivals of mice shown in (B—C). Survival statistics are Grehan-Breslow-Wilcoxon test between anti-PD1 and CIS-DPI + anti-PD1 groups. (F) Representative examples of 3 mice of the indicated groups at day 7, 14 and 21 (the same intensity scale of min-max 10^4–10^5 ph/s/cm^2/sr was used on all images for illustrative purposes and the camera was never saturated). Crosses represent mice that are no longer alive in the study at the indicated time point. (G) Percentage of responders in each group calculated as described in Fig. 1E.

The combination induced a significantly higher number of DC1 cells in the tumour, i.e., a subset specialized in tumour antigen presentation compared to the untreated whilst neither anti-PD1 or CIS-DPI alone did. Altogether, CIS-DPI combined with anti-PD1 enhanced the initiation of the anti-tumour immune response after one treatment cycle.

3.5. *Combination of CIS-DPI and anti-PD1 induces T-cell recruitment with resident -memory phenotype*

Activation and recruitment of dendritic cells are key to induce an anti-tumour immune response. DC1 sample tumour antigens in the tumour and cross-present them to T cells in the tumour-draining lymph node, resulting in T cell activation, proliferation and migration to the tumour site to exert their killing role [32]. In NSCLC patients, the presence of TILs is a predictive biomarker of anti-PD1 response [29]. To test whether recruitment of DC1 observed upon combination treatment translated into T-cell activation, TILs were characterized in the tumour at a later time point (four days) after the last treatment dose of cycle 1; i.e., day 15 (Fig. 5A). At this time point, mice had lower BLI signals (Fig. 5B-C) and tumours weighted significantly less in all treated groups compared to the untreated one (Fig. 5D).

TILs were defined by gating on TCRβ^{++} cells because we noticed the presence of a TCRβ^{+} population, which was mostly composed of CD4^{+} CD8^{+} double positive (Fig. S1C). These double-positive cells were recently shown to be present in murine and human cancers and originate from splenic T-cells upon antigen stimulation [34]. Whereas both monotherapies had marginal effects on TIL numbers, the combination treatment resulted in a significant increase in TILs (Fig. 5E). CIS-DPI administration induced a significant increase in TILs (CD3^{+}CD8^{+} quantified by IHC, Fig. 2C-D). The absence of significant difference between CIS-DPI treated and untreated tumours by flow cytometry could be due to the variability of the method involving enzymatic tissue

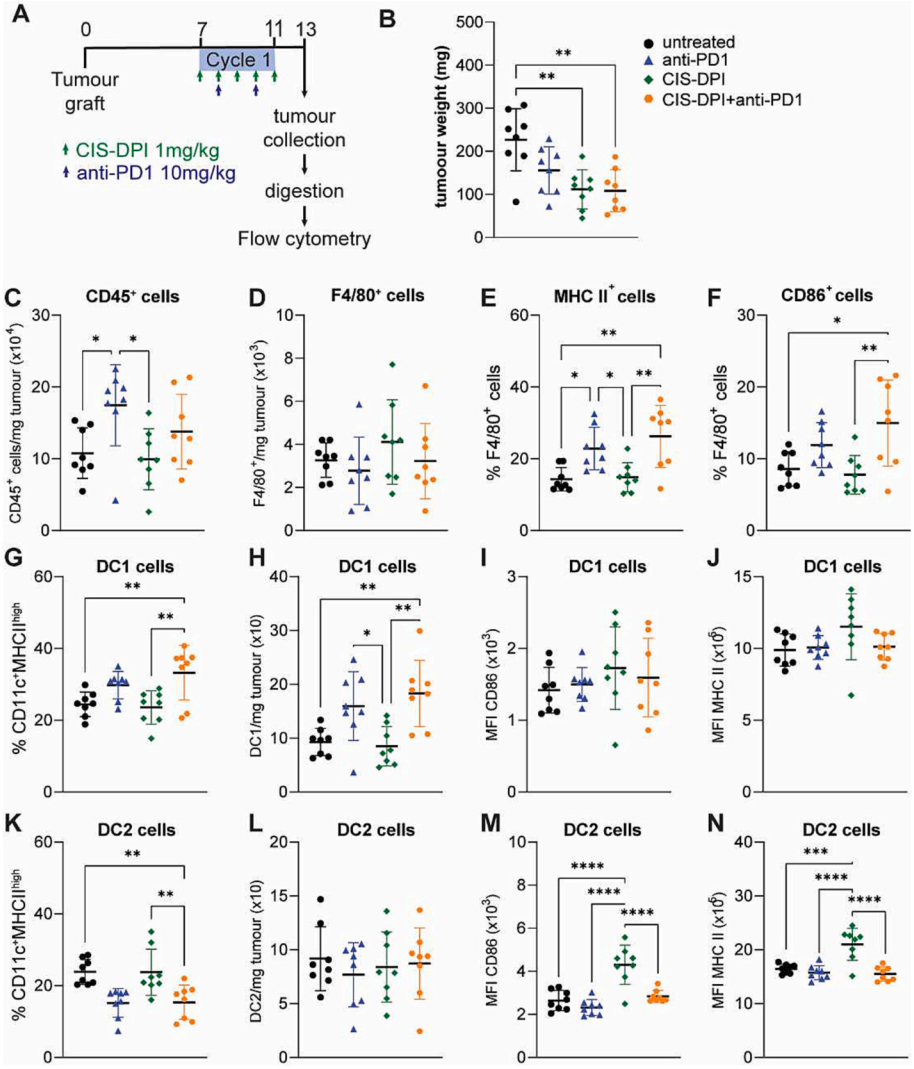

Fig. 4. CIS-DPI combined with anti-PD1 increases the number of tumour infiltrating dendritic cells. (A) Scheme of administration as explained in Fig. 3A and limited to 1 cycle. Animals were sacrificed 2 days after the last treatment dose of cycle 1. (B) Weight of M109 tumours collected on D13, 2 days after the last dose of 1 treatment cycle, $n = 10$ per group. Dots represent individual mice. (C) Number of $CD45^+$ cells per mg of tumour (gated from single live cells). (D) Number of $F4/80^+$ cells/mg of tumour (gated from $CD45^+TCR\beta^-CD19^-Ly6G^-$ cells). (*E*-F) Frequency of F4/80+ cells expressing MHC II (E) and CD86 (F). (G-J) Frequency of DC1 ($CD103^+$) among $CD11c^+MHCII^{high}$ DCs (G), their count per milligram of tumour (H) and their expression of CD86 (I) and MHC II (J). Number of $CD11c^+MHC^{high}Cd11b^+$ (DC2) per mg of tumour (G) and their expression of CD86 (H) and MHC II (I). (K—N) Frequency of DC2 ($CD11b^+$) among $CD11c^+MHCII^{high}$ DCs (K), their count per milligram of tumour (L) and their expression of CD86 (M) and MHC II (N). Statistics are one-way ANOVA, *p < 0.05, **p < 0.01, ***p < 0.001, ****$p < 0.0001$.

digestion, normalization before cell staining and acquisition or the use of a different marker to identify TILs (TCRβ by flow cytometry and CD3 for IHC). This TIL increase translated into significantly more CD8 and CD4 T cells in the combination group (Fig. 5F-J). Within the CD8 T cell population, there were significantly more proliferating $CD8^+Ki67^+$ cells in the combination group (Fig. 5H), as well as a trend toward activated $CD8^+PD1^+$ and resident memory (T_{RM}) $CD8^+CD103^+$ (Fig. G-I). NSCLC patients treated with anti-PD(L)1 therapy revealed that the density of $CD103^+CD8^+$ cells in tumours is associated with better progression-free survival [35]. Therefore, our data correlate with what is observed in the clinic, with the highest density of $CD8^+CD103^+$ in the most effective treatment group. In NSCLC, $Ki67^+PD1^+$ CD8 T cells are detected in the blood after anti-PD1 treatment and correlate with early treatment response [36]. PD1 is an immunoinhibitory receptor expressed by activated T cells and consequently the increase of $PD1^+CD8^+$ T cells characterises the anti-tumour immune response [37]. Within the CD4 T cells, there was a significant increase in the numbers of activated $CD4^+PD1^+$ cells and resident memory $CD4^+CD103^+$ with no changes in proliferating $Ki67^+$CD4 T cell population (Fig. 5K-M). In NSCLC, CD4 TILs with a resident memory phenotype ($CD4^+CD103^+$) express high levels of inhibitory receptors and are potent producers of TNF and IFNy [38]. Altogether, these data indicated a significant increase in the recruitment of proliferating ($Ki67^+$) and activated ($PD1^+$) CD4 and CD8 T-cells of T_{RM} phenotype in the combination group, with only limited effect in response to each monotherapy.

To validate these findings, we performed IHC on M109 tumours. A significant increase in $CD3^+$ cells and $CD8^+$ cells was observed in the combination CIS-DPI + anti-PD1 compared to anti-PD1 alone (Fig. 6A-B). Moreover, the immune checkpoint inhibitor PD-L1 was most significantly upregulated in the combination group compared to untreated (Fig. 6C-E). The increase of T cell infiltration was inversely correlated with the Ki67 proliferative index, which was significantly reduced in the combination group compared with the untreated and the CIS-DPI monotherapy groups (Fig. 6D-E). These data validated the infiltration of TILs upon CIS-DPI treatment and combination treatment observed by flow cytometry. Importantly, IHC is more sensitive and demonstrated a significant increase in $CD8^+$ TIL infiltration between the combination and the anti-PD1 group, validating the trend observed by flow cytometry. Our results with CIS-DPI correlates previously reported enhancing effect of cisplatin on T-cell recruitment when combined with ICI in other cancers [39,40]. In the clinic, systemic chemotherapy combined with ICIs has shown additional benefits in lung cancer as adjuvant or neoadjuvant [4,41,42]. Our preclinical results on the combination of CIS-DPI and anti-PD1 showed similar results, but with an expected better safety profile as reported in our previous studies [19,27]. Delivering cisplatin with a DPI allows the delivery of high drug doses to the lungs. Moreover, DPIs confine the cytotoxic drug before and after the dose preparation and administration (considering the drug aerosol is activated and driven into the lungs through the patient's inspiration only and drug exhalation is negligible which therefore highly

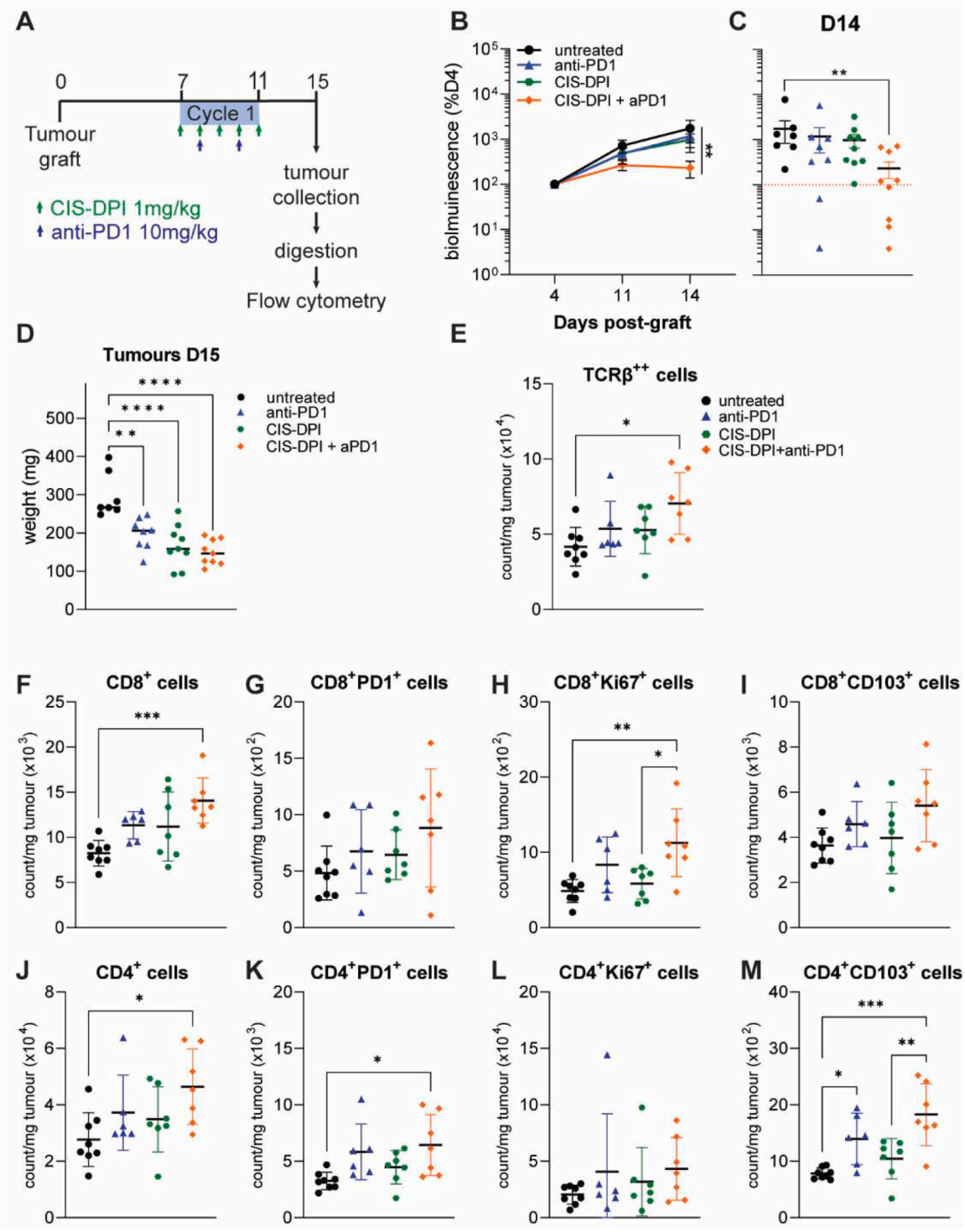

Fig. 5. CIS-DPI and anti-PD1 induces T cell recruitment. (A) Scheme of administration as explained in Fig. 3A. Animals were sacrificed 4 days after the last treatment dose of cycle 1 (day 15) and tumours were collected for analysis. (B) Tumour growth measured by bioluminescence (BLI. Dots are mean ± SEM. (C) Tumour growth (BLI) at D14, the day before tumours were collected and weighted. Dots are individual mice. (D) Weights of M109 tumours on day 15. (E) Number of TCRβ^{++} cells normalised per mg of tumour. Number of CD8^{+} cells (F) and CD4^{+} cells (J) per mg of tumour are shown. Within the CD8^{+} population, the count of cells expressing PD1 (G), Ki67 (H) and CD103 (I) was measured. Within the CD4^{+} population, the count of cells expressing PD1 (K), Ki67 (L) and CD103 (M) was measured. Statistics are two-way anova multiple comparisons (B—C) or one-way ANOVA, *p < 0.05, **p < 0.01, ***p < 0.001, ****p < 0.0001.

limit air contamination). DPIs are small, portable, and cheap, they can be tailored as disposable devices, hermetically closed after the administration procedure [43]. Thus, CIS-DPI treatment can be taken at home (and not in dedicated facilities to contain the aerosol, only possible at hospital), enabling high frequency of administration and metronomic chemotherapy. Our data demonstrated that repeated cisplatin administration favoured an immunogenic response inducing T cell recruitment, which was further enhanced by the immune checkpoint inhibitor anti-PD1.

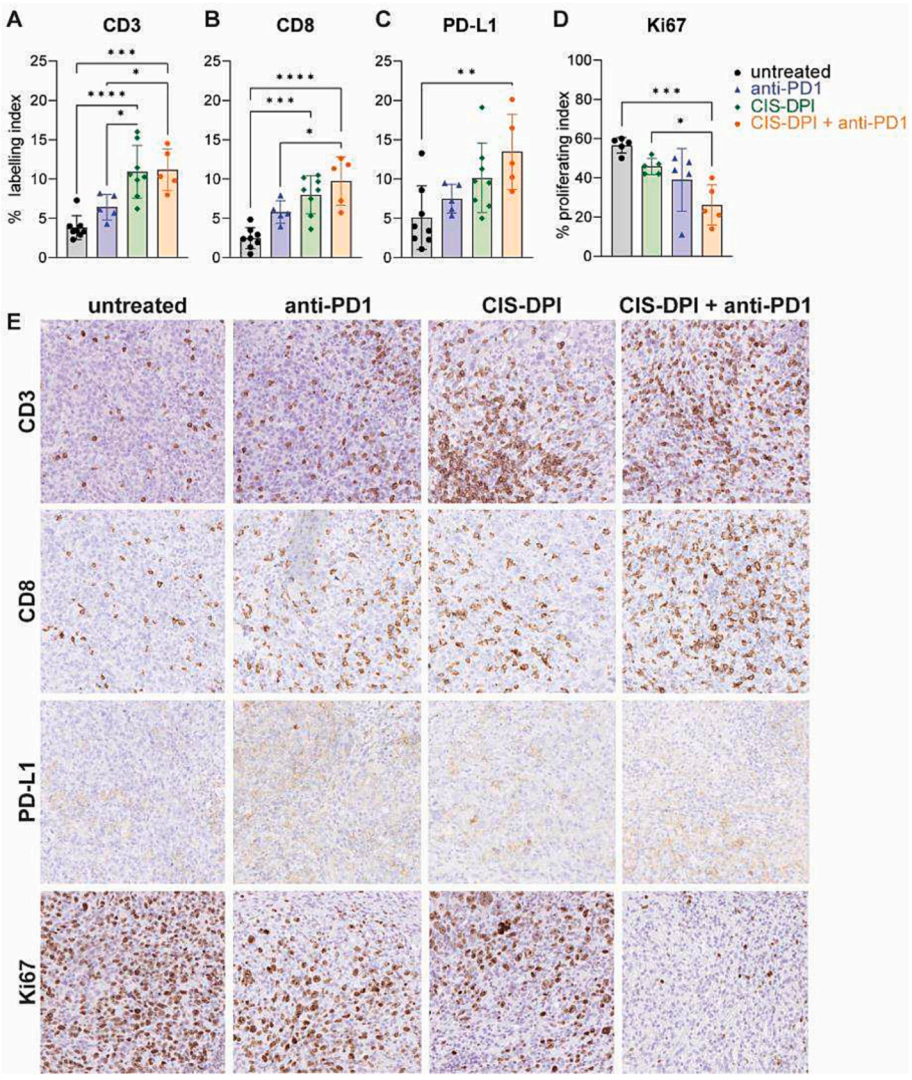

Fig. 6. Immunohistochemistry on M109 tumours on day 15 (4 days after the last treatment dose of cycle 1). Dose regimen is shown in Fig. 5A. For untreated and CIS-DPI groups, data were pooled with results shown in Fig. 2. Quantification performed as described in Fig. 2. (A) CD3, (B) CD8, and (C) PD-L1 quantification on M109 tumours. (D) Ki67 proliferating index corresponding to the percentage of $Ki67^{+}$ area in the tumour. (E) Representative images of one sample from each group for indicated marker (20× lens). Scale bar represents 100 μm. Statistics are one-way ANOVA multiple comparisons, *$p < 0.05$, **$p < 0.01$, ***$p < 0.001$, ****$p < 0.0001$.

4. Conclusions

The preclinical in vivo evaluation of CIS-DPI demonstrated a rapid cytotoxic and immunogenic effect, with its potential to be used as a novel inhalable metronomic chemotherapy. Moreover, it enhanced the anti-tumour immune response when combined with anti-PD1. This resulted in reduced tumour growth and longer survival rates over time than the anti-PD1 monotherapy. Therefore, combining CIS-DPI with ICIs, promises higher efficacy, reduced toxicities, and a better quality of life for patients who could take their treatment at home. It remains to be evaluated in the clinic which dose levels and regimens would be optimal to induce the strongest cytotoxic and immunogenic effects when combined with ICI, such as anti-PD1.

Funding

T. Davenne and this work were supported by the Région Wallonne FIRST entreprise convention 8249, a collaboration between InhaTarget Therapeutics and the U-CRI. This work was also supported by the Région Wallonne Win4Company convention 8169. The CMMI is supported by the European Regional Development Fund and the Walloon Region.

Consent for publication

All authors agreed to submit this manuscript. The graphical abstract was made with Biorender.

Declaration of Competing Interest

The authors declare the following financial interests/personal relationships which may be considered as potential competing interests: K. Amighi, N. Wauthoz, and R. Rosière are inventors of patents related to some technologies described in the paper and are co-founders of InhaTarget Therapeutics. R. Rosière is also the CSO of InhaTarget Therapeutics and a scientific collaborator of the Unit of Pharmaceutics and Biopharmaceutics. The authors have no other relevant affiliations or financial involvement with any organization or entity with a financial interest in or financial conflict with the subject matter or materials discussed in the manuscript apart from those disclosed.

Data availability

Data will be made available on request.

Acknowledgements

We would like to thank Justine Allard, Amandine Collin and Egor Zindy from the CMMI for their help with this work.

Appendix A. Supplementary data

Supplementary data to this article can be found online at https://doi.org/10.1016/j.jconrel.2022.11.055.

References

[1] R.L. Siegel, K.D. Miller, H.E. Fuchs, A. Jemal, Cancer statistics, 2022, CA Cancer J. Clin. [Internet] 72 (1) (2022 Jan 1) 7–33. Available from, https://doi.org/10.3322/caac.21708.

[2] Q. Sun, X. Wei, Z. Wang, Y. Zhu, W. Zhao, Y. Dong, Primary and Acquired Resistance against Immune Check Inhibitors in Non-Small Cell Lung Cancer, Available from: https://creativecommons.org/licenses/by/4.0/, 2022.

[3] C. Pfirschke, C. Engblom, S. Rickelt, V. Cortez-Retamozo, C. Garris, F. Pucci, et al., Immunogenic chemotherapy sensitizes tumors to checkpoint blockade therapy, Immunity [Internet] 44 (2) (2016 Feb 16) 343–354. Available from: https://doi.org/10.1016/j.immuni.2015.11.024.

[4] A.L. Desage, W. Bouleftour, O. Tiffet, P. Fournel, C. Tissot, Use of adjuvant chemotherapy in resected non-small cell lung cancer in real-life practice: a systematic review of literature Desage et al. AC in resected NSCLC, Transl. Lung Cancer Res. [Internet] 10 (12) (2021), https://doi.org/10.21037/tlcr-21-557. Available from:.

[5] E. Cella, L. Zullo, S. Marconi, G. Rossi, S. Coco, C. Dellepiane, et al., Immunotherapy-chemotherapy combinations for non-small cell lung cancer: current trends and future perspectives, Expert Opin. Biol. Ther. [Internet] (2022 Aug 22), https://doi.org/10.1080/14712598.2022.2116273 null-null. Available from:.

[6] B. Rosenberg, L. Vanvamp, T. Krigas, Inhibition of cell division in Escherichia coli by electrolysis products from a platinum electrode, Nature. 205 (1965) 698–699.

[7] S. Ghosh, Cisplatin: the first metal based anticancer drug, Bioorg. Chem. 88 (2019 Jul 1), 102925.

[8] Y. Han, P. Wen, J. Li, K. Kataoka, Targeted nanomedicine in cisplatin-based cancer therapeutics, J. Control. Rel. [Internet] 345 (2022 May 1) 709–720 [cited 2022 Jun 3]. Available from: https://linkinghub.elsevier.com/retrieve/pii/S0168365922001833.

[9] S.K. Bardal, J.E. Waechter, D.S. Martin, Neoplasia, Appl. Pharmacol. [Internet] 20 (2011) 305–324 [cited 2022 Jun 2];305–24. Available from: https://linkinghub.elsevier.com/retrieve/pii/B9781437703108000208.

[10] N. Makrilia, E. Syrigou, I. Kaklamanos, L. Manolopoulos, M.W. Saif, Hypersensitivity reactions associated with platinum antineoplastic agents: a systematic review, Metal-Based Drugs 2010 (2010).

[11] N. Wauthoz, R. Rosière, K. Amighi, Inhaled cytotoxic chemotherapy: clinical challenges, recent developments, and future prospects, Expert. Opin. Drug Deliv. [Internet] 18 (3) (2021 Mar 4) 333–354. Available from: https://doi.org/10.1080/17425247.2021.1829590.

[12] F. Lavorini, F. Buttini, O.S. Usmani, 100 years of drug delivery to the lungs, in: J. E. Barrett, C.P. Page, M.C. Michel (Eds.), Concepts and Principles of Pharmacology: 100 Years of the Handbook of Experimental Pharmacology [Internet], Springer International Publishing, Cham, 2019, pp. 143–159. Available from: https://doi.org/10.1007/164_2019_335.

[13] F. Gagnadoux, J. Hureaux, L. Vecellio, T. Urban, A. le Pape, I. Valo, et al., Aerosolized chemotherapy, J. Aerosol. Med. Pulm. Drug Deliv. [Internet] 21 (1) (2008 Mar 1) 61–70. Available from: https://doi.org/10.1089/jamp.2007.0656.

[14] K. Darwiche, P. Zarogoulidis, N.K. Karamanos, K. Domvri, E. Chatzaki, T. C. Constantinidis, et al., Efficacy versus safety concerns for aerosol chemotherapy in non-small-cell lung cancer: a future dilemma for micro-oncology, Future Oncol. [Internet] 9 (4) (2013 Apr 1) 505–525. Available from, https://doi.org/10.2217/fon.12.205.

[15] M.A. Bernabeu-Martínez, M. Ramos Merino, J.M. Santos Gago, L.M. Álvarez Sabucedo, C. Wanden-Berghe, J. Sanz-Valero, Guidelines for safe handling of hazardous drugs: a systematic review, PLoS One [Internet] 13 (5) (2018 May 11), e0197172. Available from: https://doi.org/10.1371/journal.pone.0197172.

[16] B.P.H. Wittgen, P.W.A. Kunst, K. van der Born, A.W. van Wijk, W. Perkins, F. G. Pilkiewicz, et al., Phase I study of aerosolized SLIT cisplatin in the treatment of patients with carcinoma of the lung, Clin. Cancer Res. [Internet] 13 (8) (2007 Apr 16) 2414–2421. Available from, https://doi.org/10.1158/1078-0432.CCR-06-1480.

[17] S. Chraibi, R. Rosière, L. Larbanoix, P. Gérard, I. Hennia, S. Laurent, et al., The combination of an innovative dry powder for inhalation and a standard cisplatin-based chemotherapy in view of therapeutic intensification against lung tumours, Eur. J. Pharm. Biopharm. 164 (2021 Jul 1) 93–104.

[18] V. Levet, R. Merlos, R. Rosière, K. Amighi, N. Wauthoz, Platinum pharmacokinetics in mice following inhalation of cisplatin dry powders with different release and lung retention properties, Int. J. Pharm. 517 (1–2) (2017 Jan 30) 359–372.

[19] S. Chraibi, R. Rosière, E. de Prez, M.H. Antoine, M. Remmelink, I. Langer, et al., Pulmonary and renal tolerance of cisplatin-based regimens combining intravenous and endotracheal routes for lung cancer treatment in mice, Int. J. Pharm. 599 (2021 Apr 15), 120425.

[20] N. Wauthoz, G. Bastiat, E. Moysan, A. Cieślak, K. Kondo, M. Zandecki, et al., Safe lipid nanocapsule-based gel technology to target lymph nodes and combat mediastinal metastases from an orthotopic non-small-cell lung cancer model in SCID-CB17 mice, Nanomedicine. 11 (5) (2015 Jul 1) 1237–1245.

[21] J.B. Kim, K. Urban, E. Cochran, S. Lee, A. Ang, B. Rice, et al., Non-invasive detection of a small number of bioluminescent cancer cells in vivo, PLoS One 5 (2) (2010 Feb 23), e9364.

[22] C.P.W. Klerk, R.M. Overmeer, T.M.H. Niers, H.H. Versteeg, D.J. Richel, T. Buckle, et al., Validity of bioluminescence measurements for noninvasive in vivo imaging of tumor load in small animals, Biotechniques. 43 (1 Suppl) (2007 Jul) 7–13, 30.

[23] A. Rehemtulla, L.D. Stegman, S.J. Cardozo, S. Gupta, D.E. Hall, C.H. Contag, et al., Rapid and quantitative assessment of cancer treatment response using in vivo bioluminescence imaging, Neoplasia. 2 (6) (2000) 491–495.

[24] T. Browder, C.E. Butterfield, B.M. Kräling, B. Shi, B. Marshall, M.S. O'Reilly, et al., Antiangiogenic scheduling of chemotherapy improves efficacy against experimental drug-resistant cancer, Cancer Res. 60 (7) (2000 Apr 1) 1878–1886.

[25] F.Z. Shen, J. Wang, J. Liang, K. Mu, J.Y. Hou, Y.T. Wang, et al., Low-dose metronomic chemotherapy with cisplatin: can it suppress angiogenesis in H22 hepatocarcinoma cells? Int. J. Exp. Pathol. 91 (2010) 10–16.

[26] Yefei Shu, Shanshan Weng, Song Zheng, Metronomic chemotherapy in non-small cell lung cancer, Oncol. Lett. [Internet] 20 (6) (2022) 307. Available from: http://www.

[27] S. Chraïbi, R. Rosière, E. de Prez, P. Gérard, M.H. Antoine, I. Langer, et al., Preclinical tolerance evaluation of the addition of a cisplatin-based dry powder for inhalation to the conventional carboplatin-paclitaxel doublet for treatment of non-small cell lung cancer, Biomed. Pharmacother. 139 (2021 Jul), 111716.

[28] M. Niu, M. Yi, N. Li, S. Luo, K. Wu, Predictive biomarkers of anti-PD-1/PD-L1 therapy in NSCLC, Exp. Hematol. Oncol. [Internet] 10 (1) (2021) 18. Available from: https://doi.org/10.1186/s40164-021-00211-8.

[29] K. Hummelink, V. van der Noort, M. Muller, R.D. Schouten, F. Lalezari, D. Peters, et al., PD-1T TILs as a predictive biomarker for clinical benefit to PD-1 blockade in patients with advanced NSCLC, Clin. Cancer Res. [Internet] (2022 Jul 19), https://doi.org/10.1158/1078-0432.CCR-22-0992. CCR-22-0992. Available from:.

[30] L. Fournel, Z. Wu, N. Stadler, D. Damotte, F. Lococo, G. Boulle, et al., Cisplatin increases PD-L1 expression and optimizes immune check-point blockade in non-small cell lung cancer, Cancer Lett. 464 (2019 Nov 1) 5–14.

[31] M. Niu, M. Yi, N. Li, S. Luo, K. Wu, Predictive biomarkers of anti-PD-1/PD-L1 therapy in NSCLC, Exp. Hematol. Oncol. [Internet] 10 (1) (2021) 18. Available from: https://doi.org/10.1186/s40164-021-00211-8.

[32] S.K. Wculek, F.J. Cueto, A.M. Mujal, I. Melero, M.F. Krummel, D. Sancho, Dendritic cells in cancer immunology and immunotherapy, Nat. Rev. Immunol. [Internet] 20 (1) (2020) 7–24. Available from: https://doi.org/10.1038/s41577-019-0210-z.

[33] J. Steenbrugge, J. Bellemans, N. van der Elst, K. Demeyere, J. de Vliegher, T. Perera, et al., One cisplatin dose provides durable stimulation of anti-tumor immunity and alleviates anti-PD-1 resistance in an intraductal model for triple-negative breast cancer, Oncoimmunology [Internet] 11 (1) (2022 Dec 31), 2103277. Available from: https://doi.org/10.1080/2162402X.2022.2103277.

[34] S.E. Schad, A. Chow, L. Mangarin, H. Pan, J. Zhang, N. Ceglia, et al., Tumor-induced double positive T cells display distinct lineage commitment mechanisms and functions, J. Exp. Med. [Internet] 219 (6) (2022 May 23), e20212169. Available from: https://doi.org/10.1084/jem.20212169.

[35] S. Corgnac, I. Malenica, L. Mezquita, E. Auclin, E. Voilin, J. Kacher, et al., CD103+ CD8+ TRM cells accumulate in tumors of anti-PD-1-responder lung cancer patients and are tumor-reactive lymphocytes enriched with Tc17, Cell Rep. Med. 1 (7) (2020 Oct 20), 100127.

[36] A.O. Kamphorst, R.N. Pillai, S. Yang, T.H. Nasti, R.S. Akondy, A. Wieland, et al., Proliferation of PD-1+ CD8 T cells in peripheral blood after PD-1-targeted therapy in lung cancer patients, 2022. Available from: www.pnas.org/cgi/doi/10.1073/pnas.1705327114.

[37] G.J. Freeman, A.J. Long, Y. Iwai, K. Bourque, T. Chernova, H. Nishimura, et al., Engagement of the Pd-1 Immunoinhibitory receptor by a novel B7 family member leads to negative regulation of lymphocyte activation, J. Exp. Med. [Internet] 192 (7) (2000 Oct 2) 1027–1034. Available from: https://doi.org/10.1084/jem.192.7.1027.

[38] F. Mami-Chouaib, L. Pace, B.S. Sheridan, A.E. Oja Aoja, Pleun Hombrink Phombrink Sanquinnl, D. der Zwan Van, et al., Functional heterogeneity of CD4 + tumor-infiltrating lymphocytes with a resident memory phenotype in NSCLC, Front. Immunol. 9 (2018) 2654. Available from: www.frontiersin.org.

[39] D. Wakita, T. Iwai, S. Harada, M. Suzuki, K. Yamamoto, M. Sugimoto, Cisplatin augments antitumor T-cell responses leading to a potent therapeutic effect in combination with PD-L1 blockade, Anticancer Res. [Internet] 39 (4) (2019 Apr 1) 1749. Available from: http://ar.iiarjournals.org/content/39/4/1749.abstract.

[40] W. Lin, J. Qian, H. Wang, L. Ren, Y. Yang, C. Chen, et al., Cisplatin plus anti-PD-1 antibody enhanced treatment efficacy in advanced esophageal squamous cell carcinoma, Am. J. Cancer Res. 12 (2) (2022) 451–468.

[41] J.P. Pignon, H. Tribodet, G. Scagliotti, J.Y. Douillard, F.A. Shepherd, R.J. Stephens, et al., Lung adjuvant cisplatin evaluation: a pooled analysis by the LACE collaborative group, J. Clin. Oncol. [Internet] 26 (21) (2008) 3552–3559. Available from: https://doi.org/10.1200/JCO.2007.13.9030.

[42] J. Isaacs, Thomas, E. Stinchcombe, Neoadjuvant and adjuvant systemic therapy for early-stage non-small-cell lung cancer, Drugs [Internet] 123AD (2022), https://doi.org/10.1007/s40265-022-01721-3. Available from:.

[43] R. Rosière, T. Berghmans, P. de Vuyst, K. Amighi, N. Wauthoz, Cancers the position of inhaled chemotherapy in the care of patients with lung tumors: clinical feasibility and indications according to recent pharmaceutical progresses, 2022. Available from: www.mdpi.com/journal/cancers.